Effects of end distance on thin sheet steel single shear bolted connections at elevated temperatures

Yancheng CAI [a,*],   Ben YOUNG [b]

[a] Department of Civil Engineering ,The University of Hong Kong, Pokfulam Road, Hong Kong

[b] Department of Civil and Environmental Engineering, The Hong Kong Polytechnic University, Hong Kong

Abstract

Thin sheet steel (TSS) single shear bolted connections at elevated temperatures were investigated experimentally in this study. The TSS 0.42 mm G550 and 1.90 mm G450 were used to fabricate the connection specimens. The connection specimens were designed with the variation of end distance. The specimens were tested at 5 different nominal temperature levels up to 900 °C using the steady state test method. The effects of end distance and temperature on the behaviour of bolted connections were investigated. It was found that the ultimate loads increased with the increment of the end distance up to three times the bolt diameter. Generally, the deteriorations of the connection strengths are in a similar manner to the corresponding material properties at elevated temperatures. The experimental results were compared with the predictions by using the Australian/New Zealand Standard (AS/NZS), European Code (EC3-1.3) and North American Specification (NAS) for cold-formed steel structures. In calculating the nominal strengths of the connections, the reduced material properties of TSS obtained at elevated temperatures were used. Overall, it is shown that the predictions from the AS/NZS, NAS and EC3-1.3 are conservative, with the AS/NZS providing the least conservative and least scattered predictions. However, the reliability analysis showed that the design provisions of the three design specifications are not reliable for the TSS single shear bolted connections in this study, with considerable scope for the development of improved design formulae. Generally, the AS/NZS and NAS could provide accurate predictions of failure modes for TSS connection specimens failed in tearout failure and bearing failure at different temperature levels.

Keywords: Bearing failure; bolted connection; elevated temperatures; experimental investigation; tearout failure; thin sheet steel.

---

[*] Corresponding author. Tel.: +852-2859-2665;

E-mail address: yccai@hku.hk (Y. Cai).

1. Introduction

Structural members of cold-formed steel are commonly fabricated from steel sheets by cold-rolling and brake-pressing methods. The structural behaviour of cold-formed steel members has been investigated extensively, including beams [1-2], columns [3-4], beam-columns [5-6] and built-up sections [7-9]. Bolted connections are commonly used in the design of cold-formed steel structures. Investigation of bolted connections fabricated from sheet steels were conducted by Rogers and Hancock [10-11]. They proposed design rules that covering the different failure modes of the thin sheet steel (TSS) connections, including tearout (shear out), bearing and net section tension. It should be noted that the failure mode due to short end distance (e_1) is found to be tearout failure in AS/NZS [12], and called "shear rupture" in NAS [13]. Recently, the resistance of bolted connections in cold-reduced steel sheets subjected to block shear failure (multiple bolts) was investigated by Teh and Clements [14]. Furthermore, Teh and Uz [15] carried out a series of tests on the effect of loading directions on the bearing capacity of cold-reduced steel sheets. However, it should be noted that these tests were conducted at ambient (room) temperature condition only, but not at high temperatures.

The safety design of steel structures under fire conditions is a matter of serious concern due to the deteriorations of strength and stiffness at high temperatures, which may lead to the structural collapse [16-18]. Connections are critical structural elements of building frames in fire conditions [19], e.g., bolted connections. Extensive investigations were carried out to study the behaviour of end-plate bolted connections in steel structures, where the bolts in the connections were subjected to tension and shear. These connections were carried out by both experimental and numerical studies [20-22], and numerical simulation and analytical analysis [23-27]. In addition, single high strength steel bolts subjected to combined tension and shear in fire conditions were also experimentally investigated recently. The test results showed that as the temperature rises, the strength of the bolts decreases while at the same time ductility increases [28]. The design of bolted connections in the response of steel structures under fire to avoid progressive collapse were discussed in Burgess et al. [29].

Investigations on the TSS bolted connections at high temperatures are relative limited. Yan and Young [30-31] conducted a series of tests on TSS bolted connections at elevated temperatures; based on the test results and further numerical investigations, the bearing resistance design rules were proposed for TSS double shear bolted connections at elevated temperatures [32]. End distance (e_1), namely, the distance measured in the line of force from the center of bolt hole to the nearest edge of an adjacent hole or to the end of the plate as stated in AS/NZS [12], has effects on the ultimate strength and failure mode of a bolted connection subjected to tensile loading. However, it should be noted that to date there have not been any investigations into the effects of e_1 and elevated temperatures on TSS single shear bolted connections. Furthermore, the current design specifications, such as AS/NZS [12], EC3-1.3 [33]

and NAS [13], for cold-formed steel bolted connections subjected to tensile loading are only applicable for ambient temperature condition, but not for elevated temperatures. Hence, this paper mainly focused on the structural behaviour of TSS single shear one-bolted connections with variations of end distance (e_1) at elevated temperatures, where the connection specimens were subjected to tensile loading.

In this study, the effects of e_1 on TSS single shear bolted connections at elevated temperatures were investigated experimentally using the steady state test method. The TSS 0.42 mm G550 and 1.90 mm G450 were used to fabricate the connection specimens. The connection specimens were designed in 2 series with different ratios of bolt diameter (d) to connection plate thickness (t). In each series, the e_1 of the connection specimen was varied. The specimens were tested at 5 different nominal temperature (T) levels, namely, at 22 °C (ambient temperature), 300 °C, 450 °C, 600 °C and 900 °C. The effects of e_1 and T on the behaviour of the bolted connections were obtained, including load-deflection curves, ultimate loads and failure modes. In addition, the experimental ultimate loads and failure modes were used to assess the applicability of the current design specifications for TSS bolted connections at elevated temperatures, i.e., AS/NZS [12], EC3-1.3 [33] and NAS [13]. In calculating the nominal strengths of the connections, the reduced material properties of TSS obtained at elevated temperatures were used. The reliability of the current design rules was evaluated using reliability analysis.

2.   Steady state test method

Steady state test method and transient state test method are commonly used in the tests of structures under fire condition. Generally, for the steady state test method, the specimen is heated to a predetermined temperature level, and then loaded until it fails; while for the transient state test method, the specimen is loaded to a certain level, and then heated until it fails. The former test method could be easier and safer in fire testing due to the displacement control mode used instead of load control mode in operating the testing machine. It should be noted that previous researches on the TSS bolted connections at elevated temperatures conducted by Yan and Young [31], and cold-formed stainless steel bolted connections at elevated temperatures conducted by Cai and Young [34], showed that the connection strengths decreased in a similar manner for both the steady state tests and the transient state tests. In this study, the steady state test method was adopted for the tests of the coupon specimens and connection specimens.

First, the temperature of the specimen was raised by an MTS model 653.04 high temperature furnace to a pre-determined level. During the heating process, the top end of the specimen was gripped, while the bottom end was free to expand. The heating rate of the furnace was adjusted within 40-60 °C/min, depending on the target temperature level. After reaching the pre-selected temperature level, the specimen

temperature was stabilized for a period of 8 to 15 minutes. This allowed the heat transfer in the specimen. After that, the bottom end of the specimen was gripped. A tensile load was applied to the specimen by driving the hydraulic actuator of the machine in displacement control mode. The test was conducted until the failure of the specimen; the temperature level was maintained throughout. A data acquisition system was used to record the temperatures, strains, deflections (elongations) and applied loads of the specimen at regular intervals during the test.

3. Experimental investigation

3.1 Coupon tests

The TSS 0.42 mm G550 and 1.90 mm G450 were used in this study. The TSS grade G550 had nominal thickness (t) of 0.42 mm, while that of the grade G450 was t = 1.90 mm. The material properties of the TSS at elevated temperatures were measured by coupon tests in an MTS testing machine. The TSS coupon specimens were cut in the rolling direction, and had the same dimensions as those tested by Yan and Young [30]. The tests were conducted at 5 different nominal temperature levels, namely, at 22 °C, 300 °C, 450 °C, 600 °C and 900 °C. The temperature levels were selected based on reduction trends in TSS material properties and TSS connection strengths at elevated temperatures conducted by Yan and Young [30]. An external thermocouple was contacted on the surface of the coupon at the middle to record the specimen temperature. An MTS model 632.54 F-11 high temperature axial extensometer was used to measure the strain at the gauge length of the coupon specimen. The TSS material properties at elevated temperatures were reported by Cai an Young [35], and were shown in Table 1, including the measured specimen temperatures (T_m), Young's modulus at ambient (E_r) and high temperatures (E_h), longitudinal 0.2% proof stress at ambient ($f_{0.2,r}$) and high temperatures ($f_{0.2,h}$), longitudinal ultimate strength at ambient ($f_{u,r}$) and high temperatures ($f_{u,h}$), ultimate strain at ambient ($\varepsilon_{u,r}$) and high temperatures ($\varepsilon_{u,h}$) and fracture strain at ambient ($\varepsilon_{f,r}$) and high temperatures ($\varepsilon_{f,h}$).

3.2 Design of bolted connection specimens

A total of 47 TSS single shear bolted connection specimens were designed. The connection specimens were fabricated by the TSS 0.42 mm G550 and 1.90 mm G450, where each specimen was bolted with the same plate thickness, i.e., 0.42 mm or 1.90 mm. The single shear connection specimen is bolted with two identical plates having one shear plane in the bolt. The connection plates were cut from the same batch of TSS as those for the coupon tests. The width (w) of the connection plates was kept as 50 mm. The length (L) of the connection plates was varied from 353 to 385 mm such that the assembled specimen length was maintained at 690 mm. High strength steel bolt (Grade 12.9) with corresponding washers at both sides were used in the specimen. The bolt has a nominal diameter (d) of 8 mm (M8). The nominal size of the bolt hole

(d_o) followed the AS/NZS [12] and NAS [13], where $d_o = (d + 1)$ for $d < 12$ mm. Hence, $d_o = 9$ mm was used in this study. The specimens were designed by varying the value of e_1, namely, $e_1 = d$, $2d$, $3d$ and $5d$. It should be noted that the minimum requirement of e_1 for bolted connection specimen is $e_1 \geq 1.5d$ in AS/NZS [12] and NAS [13], or $e_1 \geq 1.5d_o$ in EC3-1.3 [33]. Fig. 1 illustrates the definitions of symbols and values in the TSS plate.

3.3 Labeling of bolted connection specimens

The TSS single shear bolted connection specimens were divided into two groups by the nominal value of d/t, namely, $d/t = 19.05$ for 0.42 mm G550 and $d/t = 4.21$ for 1.90 mm G450. In each group, there are four series of specimens by the variation of e_1, i.e., $e_1 = d$, $2d$, $3d$ and $5d$. Each specimen series was tested at 5 different nominal temperature levels as those for the coupon tests, namely, at 22 °C, 300 °C, 450 °C, 600 °C and 900 °C. Hence, the effects of e_1 and T on the behaviour of single shear bolted connections could be obtained. Table 2 summarizes the design of the TSS single shear bolted connection specimens. The specimens were generally labelled by three segments such that the connection plate thickness (t), connection type and e_1 could be identified. For example in Table 3, the first segment "042" and "190" stand for the TSS of 042 mm G550 and 1.90 mm G450, respectively; "S" is short for single shear bolted connection; and the third segment shows the value of e_1. The last number "r" indicates it is a repeated test.

3.4 Tests of single shear bolted connections

Tests of TSS single shear bolted connections were conducted in the same MTS machine as for coupon tests. At ambient temperature condition, two linear voltage differential transducers (LVDTs) were used to measure the deflection (elongation) that covered a distance of 200 mm in the middle part of the specimen (See Figs. 2(a)-(b)). At high temperature conditions, the LVDTs were removed, instead, the aforementioned high temperature furnace was used to raise the specimen temperature (See Figs. 3(a)-(b)). The readings from the stroke of the machine were used as the specimen deflection. Note that at high temperatures, the deflection of the connection specimen mainly occurred in the high temperature zone, which was inside the furnace with the length of around 200 mm. Similar to the coupon tests, an external thermocouple was used to measure the connection specimen temperature. The location of the external thermocouple was in the vicinity of the bolt in the connection part, as shown in Fig. 3(a). The specimen was assembled into a gripping apparatus that could provide pin-end boundary conditions at each end [30, 36]. Fig. 2(a) illustrates the schematic view of the test setup. The gripping apparatus was designed such that the tensile loading was applied through the shear plane of the bolts in the connection specimens. The curling up, i.e., the sheet curls out-of-plate that deformed back towards the bolt [37] as shown in Fig. 4, at the connection part was prevented by clips linked with iron wire (see Fig. 2(a)), which was adopted by Rogers and Hancock

[10] and Yan and Young [30]. As mentioned previously, the steady state test method was used for the single shear bolted connection tests at elevated temperatures.

3.5 Test results of single shear bolted connections

The behaviour of the TSS single shear bolted connection specimens was obtained, including the relationship between the applied loads and deflections during the tests, specimen temperatures (T_m), ultimate loads (P_u) and failure modes. Figs. 5-8 illustrate the respective load-deflection curves of the specimen series 042-S-2d, 042-S-5d 190-S-2d and 190-S-5d at elevated temperatures, respectively. The horizontal axis plots the deflection of the specimens, while the vertical axis shows the corresponding applied load during the tests. The ultimate loads of the specimen at ambient temperature ($P_{u,r}$) and high temperature ($P_{u,h}$) conditions are shown in Tables 3-7. The measured T_m and the test failure modes are also reported in the tables. In this study, the test failure modes were tearout failure (T), bearing failure (B) and bolt shear (BS). Tearout failure usually occurs in bolted connections where the end distance (e_1) from the center of the bolt hole to the end of the specimen is small. Some piling of the sheet steel occurs in front of the bolt with two near-longitudinal tears extending from the piled material to the end of the specimen [37], as illustrated in Figs. 9(a)-(b) and Figs. 10(a)-(b). This leads to the characteristic of deformation at the end of the steel plate happens at the peak load due to the short end distance. TSS bolted connections fail by bearing exhibit initial tears in the direction of loading, with piling of the sheet steel in front of the bolt, which is similar to that observed for end tearout [37], as illustrated Figs. 9(c)-(d) and Figs. 10(c)-(d). There is no necking across the width of the test specimens for both tearout and bearing failure modes. The characteristics of the failure modes for TSS bolted connections are detailed in Rogers and Hancock [37] and Yan and Young [30].

4. Effects of end distance

4.1 Ultimate loads

The effects of e_1 on the ultimate load of the TSS bolted connections at different nominal temperature levels were investigated. Figs. 11-12 plot the ultimate load ($P_{u,r}$ and $P_{u,h}$) against the variations of e_1 for the connections series 042-S and 190-S, respectively. The vertical axes of the graphs show the ultimate load of each test, where the $P_{u,r}$ and $P_{u,h}$ mean the ultimate loads at ambient temperature and high temperatures, respectively. The horizontal axes plot the ratio of e_1/d for the purpose of direct comparison. For both specimen series 042-S and 190-S, it is shown that the $P_{u,r}$ and $P_{u,h}$ increase obviously with the increment of e_1/d from 1 to 5 at different nominal temperature levels. At each temperature level, the increments of $P_{u,r}$ and $P_{u,h}$ are larger from $e_1/d = 1$ to $e_1/d = 2$ than from $e_1/d = 2$ to $e_1/d = 3$. The $P_{u,r}$ and $P_{u,h}$ are generally maintained when the values of e_1/d increase from 3 to 5. This may indicate that for TSS single shear bolted connections, the $P_{u,r}$ and $P_{u,h}$ are generally maintained when

the $e_1 \geq 3d$.

4.2 Failure modes

The test failure modes of the TSS single shear connection specimens at different nominal temperatures are shown in Tables 3-7. Each table includes the specimen series tested at the same nominal temperature levels. For specimen series 042-S and 190-S tested at ambient temperature condition (see Table 3), all the connection specimen series failed in tearout (T) with $e_1 = d$ and $e_1 = 2d$ (See Fig. 9(a)-(b) and Fig. 10(a)-(b)). The characteristics of tearout at the end of the plates were not observed for $e_1 = 3d$ and $e_1 = 5d$, instead, the pure bearing failure mode was observed.

For specimen Series 042-S at the same high temperature levels, the above failure modes were similarly observed, i.e., at the nominal temperature of 300 °C, 450 °C and 600 °C and 900 °C (see Tables 4-7). While for specimen Series 190-S, the aforementioned failure modes at ambient temperature were also similarly observed at the nominal temperature of 300 °C, 450 °C and 600 °C. However, the specimens failed in bolt shear (BS) at 900 °C when the $e_1 = 2d$, $3d$ and $6d$ (see Table 7). The specimens changed the failure modes from tearout or bearing to bolt shear at higher temperature levels may be due to the larger bearing factors achieved at higher temperature levels [32] and the deteriorations of material properties of bolts are worse than those of TSS at the temperature level of 900 °C. Hence, for the same specimen series, the tearout strength or bearing strength as the minimum at the ambient temperature condition could not be the case at higher temperatures. Figs. 9-10 illustrate the failure modes of specimen series 042-S and 190-S at ambient temperature condition. Figs. 13-16 show the failure modes of specimen series 042-S-d, 042-S-3d, 190-S-d and 190-S-3d at elevated temperatures, respectively.

5. Effects of temperature

5.1 Ultimate loads

The effects of T on the $P_{u,r}$ and $P_{u,h}$ of the TSS single shear bolted connections were investigated, where the e_1 in each specimen series was maintained. It was found that the ultimate loads ($P_{u,r}$ and $P_{u,h}$) decreased as the temperature increased for both specimen series 042-S and 190-S under the same values of e_1/d, as shown in Figs. 11-12. For the purpose of direct comparison, the strength reduction for each specimen series with the same e_1 at elevated temperatures was obtained by the ratio $P_{u,h}/P_{u,r}$. The values of the ratio $P_{u,h}/P_{u,r}$ are plotted in the vertical axes of Figs. 17-18, for the specimen series 042-S and 190-S, respectively; while the horizontal axes of the figures show the specimen temperatures. In each figure, the corresponding reduction factors of material properties ($f_{0.2,h}/f_{0.2,r}$ and $f_{u,h}/f_{u,r}$) at elevated temperatures are included.

It was found that, for both specimen series, the reduction trends were similar at elevated temperatures, except for specimen Series 042-S-d at the temperature levels of 450 °C and 600 °C and Specimen 190-S-d at the temperature level of 450 °C, where smaller reduction was found. This may indicate that the effects of temperature on the strength reduction, i.e., $P_{u,h}/P_{u,r}$, are generally similar for specimen series with the same value of e_1. The reduction trends of the ultimate loads ($P_{u,h}$ and $P_{u,r}$) are generally similar to those of the corresponding $f_{0.2,h}/f_{0.2,r}$ and $f_{u,h}/f_{u,r}$ (see Figs. 17-18). The reduction factors of $f_{0.2,h}/f_{0.2,r}$ and $f_{u,h}/f_{u,r}$ generally provide conservative predictions of $P_{u,h}/P_{u,r}$ for both specimen series 042-S and 190-S with different values of e_1, except for specimen series 042-S and 190-S at the temperature level of 300 °C.

5.2 Failure modes

As discussed earlier, the failure modes of the TSS connection specimens at elevated temperatures are shown in Tables 3-7. It is shown that specimen series 042-S-d, 042-S-2d, 190-S-d and 190-S-2d failed in tearout failure mode at elevated temperatures, except for specimens of 190-S-2d, 190-S-3d and 190-S-5d at the temperature level of 900 °C. This may indicate that the effects of temperature are little on the failure modes of TSS single shear bolted connections in this study. As discussed previously, the failure mode of specimens 190-S-2d, 190-S-3d and 190-S-5d changed from tearout or bearing to bolt shear at the temperature level of 900 °C may be due to the larger bearing factors achieved at higher temperature levels [32] and the deteriorations of material properties of the bolts are worse than those of TSS at the temperature level of 900 °C. Hence, for the same specimen series, the tearout strength or bearing strength as the minimum at the ambient temperature condition could not be the case at high temperatures, which lead to the change of failure modes at elevated temperatures. It should be noted that bolt shear failure was deliberately avoided in designing the specimens at ambient temperature condition.

6. Comparison of test results with predictions

6.1 Design rules

Design rules for cold-formed steel bolted connections are available in the current specifications, i.e., the AS/NZS [12], EC3-1.3 [33] and NAS [13]. These design rules are used to calculate the nominal strengths (unfactored design strengths) of the specimens in this study. It should be noted that these design rules are applicable to ambient temperature condition only, but not for elevated temperatures. For the purpose of direct comparison and assessment, the material properties at ambient temperature were replaced by those at high temperatures in the calculation.

Different failure modes are associated with the different design equations in the current specifications [12-13, 33]. The minimum nominal strength is taken as the predicted strength of a bolted connection, and correspondingly, the predicted failure

mode. Note that a bolted connection specimen subjected to tensile loading may fail in the bolt by shear, or fail in the connection plate by bearing, tearout (shear rupture) or net section tension (tension rupture). The calculations of bolted connection specimens failed due to tearout, net section tension and bearing plate bearing are provided in Clauses 5.3.2-5.3.4 in the AS/NZS [12]. It should be noted that the rules in AS/NZS [12] apply for connection plate thicknesses between 0.42 mm and 4.76 mm. In addition, the net section tension strength is also governed by Clause 3.2.2 in the AS/NZS [12]. For the EC3-1.3 [33], the calculations for bolted connections loaded in shear are provided in Table 8.4 of Section 8.3. Note that the strength corresponding to tearout failure is incorporated into the design of bearing by the coefficient of α_b, where the effect of $e_1/(3d)$ is considered. Therefore, the EC3-1.3 [33] does not provide the tearout (shear rupture) failure. For the NAS [13], Section J3.3 specifies the designs for plate bearing failure, Section J6.1 for shear rupture and Section J6.2 for tension rupture. It should be noted that NAS [13] considers the net end distance (e_{net}) instead of e_1 in the shear rupture calculation.

It should be noted that bearing strength with consideration of bolt hole deformation was not considered in the present study. The bearing strength with consideration of bolt hole deformation is specified in the Eq. 5.3.4.3 in Section 5.3.4.3 of the AS/NZS [12] and the Eq. J3.3.2-1 in Section J3.3.2 of the NAS [13]. In addition, The TSS 0.42 mm G550 in this study is outside the lowest bound, namely, the 0.75 mm in the range of validity in the EC3-1.3 [33], and also outside the limit of no less than 0.61 mm specified in the bearing strength design in NAS [13]. However, the design equations are used for TSS 0.42 mm G550 as a direct comparison. The differences between these design rules in different specifications are detailed in Cai and Young [38].

The experimental results at elevated temperatures were compared with the predicted results by the cold-formed steel design specifications [12-13, 33] in terms of connection strengths and failure modes. In the calculation of predicted strengths, the design rules as discussed previous were used. Note that these design rules are applicable to ambient temperature condition only, but not for elevated temperatures. Hence, the material properties at ambient temperature were directly replaced by those at high temperatures in the calculation. In addition, since this study mainly focuses on the TSS bolted connections at elevated temperatures, hence, the reduced material properties due to the steel sheet thickness or ductility that required in AS/NZS [12] and NAS [13] at ambient temperature condition were not considered in the strength calculations.

6.2 Comparison of test and predicted strengths

The predicted strength was determined by the minimum nominal strength of a bolted connection by considering different failure modes, except for the failure of bolts. Note that bolt shear failure was deliberately avoided in the specimen design and

this failure mode was not observed in the test results, except for specimens 190-S-2d, 190-S-3d and 190-S-5d at 900 °C. The specimens that failed in bolt shear were not included in the strength comparisons. Tables 3-7 show the comparisons between the ultimate loads ($P_{u,r}$ and $P_{u,h}$) from tests and the predicted strengths at different nominal temperature levels. Table 8 summarizes the comparison of the ultimate loads from the tests with those from the predictions [12-13, 33]. In addition, the test results of $P_{u,r}/f_{u,r}dt$ and $P_{u,h}/f_{u,h}dt$ are plotted with the predicted curves from the specifications [12-13, 33] in Figs. 19-20, for specimen Series 042-S and 190-S, respectively.

Generally, it was found that the predictions from the EC3-1.3 [33] and NAS [13] are conservative for TSS single shear bolted connections at elevated temperatures, in particular at the temperature level of 600 °C. The EC3-1.3 [33] provides more conservative but less scattered predictions at elevated temperatures, as shown in Tables 3-7. For example (See Table 3 at 22 °C), the mean values of $P_{u,r}/P_{NAS}$ and $P_{u,r}/P_{EC}$ are 1.14 and 1.24, respectively; with the corresponding coefficient of variation (COV) of 0.262 and 0.142. However, the AS/NZS [12] generally provides unconservative predictions for connections at the nominal temperature levels of 22 °C and 300 °C, for example, the mean value and COV of $P_{u,h}P_{AS/NZS}$ at 300 °C are 0.90 and 0.093, respectively. While at high temperature levels of 450 °C, 600 °C and 900 °C, the predictions by AS/NZS [12] become conservative, where the predictions are less conservative and less scattered than those predicted by EC3-1.3 [33] and NAS [13] at the same temperature level (See Tables 5-7). For example (See Table 6 at 600 °C), the mean values of $P_{u,r}/P_{AS/NZS}$, $P_{u,r}/P_{NAS}$ and $P_{u,r}/P_{EC}$ are 1.65, 2.14 and 2.25, respectively, with the corresponding COV of 0.429, 0.767 and 0.583. Overall, the AS/NZS [12] provides the least conservative and least scattered predictions for TSS single shear bolted connections at elevated temperatures, as shown in Table 8.

6.3. Reliability analysis

Reliability analysis was performed for the TSS bolted connection design rules used in this study. The analysis was conducted in accordance with those specified in the North American Specification (NAS) for the Design of Cold-Formed Steel Structural Members [13]. The aforementioned bolted connection design provisions in the AS/NZS [12], EC3-1.3 [33] and NAS [13] were examined. It should be noted that Section A.6 of the EC3-1.3 [33] provides the procedure for evaluation of test results. For direct comparison, the reliability analysis that specified in the NAS [13] was used in this study.

In the present study, the reliability index (β) greater than or equal to 3.5 as specified in Section K2.1 of the NAS [13] was set for the design provisions being considered reliable and probabilistically safe. The resistance factors (ϕ) for bolted connection strength design as recommended by the AS/NZS [12], EC3-1.3 [33] and NAS [13] are shown in Table 8. They were used in the calculation of the reliability index (β). It should be noted that different resistance factors are specified for bolted connections subjected to different failure modes [12-13], e.g., 0.6 and 0.9 for the

failure modes of bearing and net section tension, respectively [12]. The resistance factor of 0.6 was used in the reliability analysis for both AS/NZS [12] and NAS [13]. This is because the present study is mainly focused on the TSS bolted connections subjected to failure modes of tearout and bearing, which are also the main failure modes predicted by AS/NZS [12] and NAS [13], as detailed in Section 6.4 of this paper. The resistance factor of 0.8, which is 1/1.25, was used for EC3-1.3 [33]. This resistance factor is specified in Table 8.4 of the EC3-1.3 [33] for different failure modes of bolted connections. In addition, the load combinations of 1.2DL + 1.5LL [39], 1.35DL + 1.5LL [40] and 1.2DL + 1.6LL [13] were used for the design provisions of AS/NZS [12], EC3-1.3 [33] and NAS [13], respectively; where DL represents the dead load while LL represents the live load. The ratio of 0.2 was used for DL/LL. The statistical parameters suggested in Section 6.2 of the NAS [13] were used, where $M_m = 1.10$, $F_m = 1.00$, $V_M = 0.08$ and $V_F = 0.05$, which are the mean values and coefficients of variation of material factor and fabrication factor, respectively. In addition, the mean value (P_m) and the coefficients of variation (V_P) of tests to the design prediction ratios are shown in Table 8. A correction factor (C_P) in the Section K2.1 of the NAS [13] was used to take into consideration of the influence of limited number of test data, where $C_P = (1+1/n)m/(m-2)$, in which n is the number of tests and $m = n-1$ is the degrees of freedom. The reliability index (β) for the TSS single shear and double shear bolted connections were calculated, and reported in Table 8.

It was found that the design provisions of AS/NZS [12], EC3-1.3 [33] and NAS [13] are not reliable and probabilistically not safe for TSS single shear bolted connections, as evident by the value of β_1 less than 3.5 (the values of $_1$ were calculated based on the values of ϕ_1), although it has been shown that the predictions by AS/NZS [12], EC3-1.3 [33] and NAS [13] are generally conservative with the mean values of test to predictions greater than 1.0. This may be due to the relatively large values of COV in the predictions [12-13, 33], e.g., 0.397, 0.509 and 0.669 for AS/NZS [12], EC3-1.3 [33] and NAS [13], respectively. For the purpose of direct comparison, a constant resistance factor of 0.60 ($\phi_2 = 0.6$) and a load combination of 1.2DL +1.6LL as specified in the NAS [13] were used to calculate the reliability index (β), as illustrated by β_2 in Table 8. It is shown that the design provisions of AS/NZS [12] and EC3-1.3 [33] are more reliable and probabilistically safer due to the increased values of β, e.g., the β increased from $\beta_1 = 2.09$ to $\beta_2 = 2.66$ due to the reduced resistance factor for EC3-1.3 [33]. The design provisions of AS/NZS [12] and EC3-1.3 [33] are more reliable and probabilistically safer than those of NAS [13]. However, all the design provisions [12-13, 33] are not reliable and probabilistically not safe.

6.4 Comparison of test and predicted failure modes

The failure mode associated with the predicted nominal strength for each specimen was taken as the predicted failure mode. Tables 3-7 show the corresponding

predicted failure modes from the specifications [12-13, 33] at different nominal temperature levels. As discussed previously, the effects of e_1 on the bolted connection strength is inclusively incorporated in the strength calculation of bearing failure by the coefficient of α_b in the EC3-1.3 [33]. Hence, EC3-1.3 [33] does not distinguish the tearout failure and bearing failure, but predicts the failure mode of bearing only. However, the AS/NZS [12] and NAS [13] provide tearout (shear fracture) failure and bearing failure modes.

The accuracy of the predicted failure modes were assessed by comparing with the failure modes from the tests, as shown in Tables 3-7. For the AS/NZS [12] and NAS [13], it is shown that the predictions are accurate for both specimen series (042-S and 190-S) at ambient temperature condition. Furthermore, the predicted failure modes are generally accurate for both specimen series at different high temperature levels. It should be noted that for Specimen 190-S-3d, the nominal strengths of bearing and tearout predicted by AS/NZS [12] are the same, due to the bearing factor of 3.0 was used in the bearing strength calculation by $3.0dtf_u$, which equals to the tearout strength calculation by te_1f_u, where $e_1 = 3.0d$; hence, the predictions include the two failure modes of tearout and bearing. The specimens 190-S-2d, 190-S-3d and 190-S-5d failed in bolt shear at 900 °C which was not predicted by specifications. As explained previously, bolt shear strengths were not considered in the predictions as this study mainly focuses on the failure of connection plates. Bolt shear failure was deliberately avoided in the specimen design at ambient temperature condition. Generally, the AS/NZS [12] and NAS [13] could accurately predict the specimens failed in tearout and bearing at different temperature levels. However, for the EC3-1.3 [33], only the bearing failure mode was predicted for all the specimen series at different temperature levels.

7 Conclusions

Totally 47 specimens were designed and tested to investigate the effects of end distance (e_1) and temperature (T) on thin sheet steel (TSS) single shear bolted connections. The connection specimens were fabricated by TSS 0.42 mm G550 and 1.90 mm G450. The connection specimens were designed in two series with different ratios of bolt diameter (d) to connection plate thickness (t). In each series, the e_1 of the connection specimen was varied as 1.0d, 2d, 3d and 5d. The specimens were tested by using steady state test method at 5 different nominal temperature levels, namely, at 22 °C (ambient temperature), 300 °C, 450 °C, 600 °C and 900 °C. The effects of end distance and temperature on the behaviour of the connections were obtained, including the load-deflection curves, ultimate loads and failure modes. Findings from the experimental investigations are summarized below:

- It was found that ultimate loads increase obviously with the increment of e_1/d from 1 to 3 at elevated temperatures.

- At each temperature level, the increments of ultimate loads are larger from $e_1/d = 1$ to $e_1/d = 2$ than those from $e_1/d = 2$ to $e_1/d = 3$. The ultimate loads are generally maintained when the values of e_1/d increase from 3 to 5.
- The effects of temperature on the strength reduction are generally similar for connection specimen series with the same value of e_1.
- The reduction trends of the ultimate loads ($P_{u,h}$ and $P_{u,r}$) are generally in the similar manner as those of the corresponding material properties of $f_{0.2,h}/f_{0.2,r}$ for 0.2% proof stress and $f_{u,h}/f_{u,r}$ for ultimate strength.
- The reduction factors of $f_{0.2,h}/f_{0.2,r}$ and $f_{u,h}/f_{u,r}$ generally provide a conservative predictions of $P_{u,h}/P_{u,r}$, except for specimen series 042-S and 190-S at the temperature level of 300 °C.
- All the connection specimen series failed in tearout with $e_1 = d$ and $e_1 = 2d$ at different temperature levels, except for Specimens 190-S-2d at the temperature level of 900 °C. Generally, the specimens failed in plate bearing with $e_1 = 3d$ and $e_1 = 5d$ at elevated temperatures.

The experimental results were compared with the predicted nominal strengths and failure modes by using the Australian/New Zealand Standard (AS/NZS) [12], European Code (EC3-1.3) [33] and North American Specification (NAS) [13] for cold-formed steel structures. In the calculation of predicted strengths, the material properties at ambient temperature were directly replaced by those at elevated temperatures. Findings of the comparisons are summarized below:

- The predictions from the AS/NZS [12], EC3-1.3 [33] and NAS [13] are overall conservative for TSS single shear bolted connections at elevated temperatures.
- The AS/NZS [12] provides the least conservative and least scattered predictions, while the NAS [13] provides less conservative but more scattered predictions than EC3-1.3 [33].
- Generally, the AS/NZS [12] and NAS [13] are able to provide accurate predictions of failure modes for TSS single shear bolted connection specimens at different temperature levels, except for those specimens failed in bolt shear.
- Reliability analysis showed that the design provisions of AS/NZS [12], EC3-1.3 [33] and NAS [13] are not reliable for TSS single shear bolted connections at elevated temperatures in this study.

References

[1] L. Laím, J.P.C. Rodrigues, L.S. da Silva, Experimental and numerical analysis on the structural behaviour of cold-formed steel beams, Thin-Walled Structures. (2013) 1–13.

[2] L. Wang, B. Young, Design of cold-formed steel channels with stiffened webs subjected to bending, Thin Walled Structures. 85 (2014) 81-92.

[3] B. Young, G.J. Hancock, Compression tests of channels with inclined simple edge stiffeners, Journal of Structural Engineering. 129(10) (2003) 1403–1411.

[4] B. Young, K.J.R. Rasmussen, Design of lipped channel columns, Journal of Structural Engineering. 124(2) (1998) 140–148.

[5] S. Torabian, B. Zheng, B.W. Schafer, Experimental response of cold-formed steel lipped channel beam-columns, Thin-Walled Structures. 89 (2015) 152–168.

[6] S. Torabian, D.C. Fratamico, B.W. Schafer, Experimental response of cold-formed steel Zee-section beam-columns, Thin-Walled Structures. 98 (2016) 496-517.

[7] L. Wang, B. Young, Behavior of Cold-Formed Steel Built-Up Sections with Intermediate Stiffeners under Bending. I: Tests and Numerical Validation, Journal of Structural Engineering. 142(3) (2016) 04015150-1-9.

[8] L. Wang, B. Young, Behavior of Cold-Formed Steel Built-Up Sections with Intermediate Stiffeners under Bending. II: Parametric Study and Design, Journal of Structural Engineering. 142(3) (2016) 04015151-1-11.

[9] D. C. Fratamico, S. Torabian, X. Zhao, K.J.R. Rasmussen, B.W. Schafer, Experiments on the global buckling and collapse of built-up cold-formed steel columns, Journal of Constructional Steel Research. 144 (2018) 65–80.

[10] C.A. Rogers, G.J. Hancock, Bolted connection tests of thin G550 and G300 sheet steels, Journal of Structural Engineering. 124(7) (1998) 798–808.

[11] C.A. Rogers, G.J. Hancock, Bolted connection design for sheet steels less than 1.0 mm thick, Journal of Constructional Steel Research. 51 (1999) 123–146.

[12] AS/NZS, Cold-formed Steel Structures." Australian/New Zealand Standard, AS/NZS4600:2018, Sydney, Australia, Standards Australia, 2018.

[13] NAS, North American Specification for the Design of Cold-Formed Steel Structural Members, American Iron and Steel Institute, AISIS100-2016, AISI Standard, 2016.

[14] L.H. Teh, D.D.A. Clements, Block shear capacity of bolted connections in cold-reduced steel sheets, Journal of Structural Engineering. 138(4) (2012) 459–67.

[15] L.H. Teh, M.E. Uz, Effect of loading direction on the bearing capacity of cold-reduced steel sheets, Journal of Structural Engineering. 140 (2014) 06014005-1-5.

[16] R. Sun, Z. Huang, I.W. Burgess, Progressive collapse analysis of steel structures under fire conditions, Engineering Structures. 34 (2012), 400-413

[17] R. Sun, Z. Huang, I.W. Burgess, The collapse behaviour of braced steel frames exposed to fire, Journal of Constructional Steel Research. 72 (2012), 130-142

[18] R. Sun, I.W. Burgess, Z. Huang, G. Dong, Progressive failure modelling and ductility demand of steel beam-to-column connections in fire, Engineering Structures.

89 (2015), 66-78

[19] F. Wald , L. Simo˜es da Silva, D.B. Moore, T. Lennon, M. Chladna´, A. Santiago, M. Benesˇ, L. Borges, Experimental behaviour of a steel structure under natural fire, Fire Safety Journal. 41 (2006), 509–522.

[20] W.Y. Wang, G.Q. Li, Y.L. Dong, Experimental study and spring-component modeling of extended end-plate joints in fire. J Constr Steel Res. 63(2007),1127–37.

[21] H. Yu, I.W. Burgess, J. Davison, R.J. Plank, Experimental and numerical investigations of the behavior of flush end plate connections at elevated temperatures. J Struct Eng. 137(2011),80–87.

[22] Y. Gao, H. Yu, G. Shi, Resistance of flush endplate connection under tension and shear in fire. J Constr Steel Res. 86 (2013), 195–205

[23] K.S. Al-Jabri, A Seibi, A Karrech, Modelling of unstiffened flush end-plate bolted connections in fire. Journal of Constructional Steel Research. 62 (2006), 151–159.

[24] F.M. Block, I.W. Burgess, J.B. Davison, R.J. Plank, The development of a component-based connection element for endplate connections in fire, Fire Safety Journal. 42 (2007), 98–506.

[25] H. Yu, I.W. Burgess, J.B. Davison, R.J. Plank, Numerical simulation of bolted steel connections in fire using explicit dynamic analysis. Journal of Constructional Steel Research. 64 (2008), 515–525.

[26] M.E. Garlock, S. Selamet, Modeling and behavior of steel plate connections subject to various fire scenarios, Journal of Structural Engineering. 136(7) (2010), 897-906.

[27] R. Rahnavard, R.J. Thomas, Numerical evaluation of the effects of fire on steel connections; Part 1: simulation Techniques, Case Stud. Therm. Eng. 12 (2019), 445–453.

[28] J. Lange, A. Kawohl, Tension-shear interaction of high-strength bolts during and after fire. Steel Construction. 12(2) (2019), 124-134.

[29] I.W. Burgess, J.B. Davison, G. Dong, S. Huang, The role of connections in the response of steel frames to fire. Structural Engineering Structural Engineering International. 22(4) (2012), 449-461

[30] S. Yan, B. Young, Tests of single shear bolted connections of thin sheet steels at elevated temperatures - Part I: steady state tests, Thin-Walled Structures. 49 (2011) 1320–33.

[31] S. Yan, B. Young, Effects of Elevated Temperatures on Double Shear Bolted Connections of Thin Sheet Steels, Journal of Structural Engineering. 139 (2013) 757-771.

[32] S. Yan, B. Young, Bearing factors for single shear bolted connections of thin sheet steels at elevated temperatures, Thin-Walled Structures. 52 (2012) 126–142.

[33] EC3-1.3, Eurocode3—Design of Steel Structures—Part 1–3: General Rules Supplementary Rules for Cold-formed Members and Sheeting, Brussels: European Committee for Standardization, EN1993-1-3:2006, 2006.

[34] Y. Cai, B. Young, High temperature tests of cold-formed stainless steel double shear bolted connections, Journal of Constructional Steel Research. 104 (2015) 49-63.

[35] Y. Cai, B. Young, Effects of end distance on thin sheet steel double shear bolted

connections at elevated temperatures, ASCE – Journal of Structural Engineering. 2019, (Accepted).

[36] Y. Cai, B. Young, Structural behavior of cold-formed stainless steel bolted connections, Thin-Walled Structures. 83 (2014) 147-156.

[37] C.A. Rogers, and G.J. Hancock, Failure modes of bolted-sheet-steel connections loaded in shear. Journal of Structural Engineering ASCE 2000; 126(3): 288-296.

[38] Y. Cai, B. Young, Effects of end distance on thin sheet steel bolted connections, Engineering Structures. 196 (2019), 109331.

[39] AS/NZS 1170. Structural design actions. Part 0: General principles. Australian/New Zealand Standard, AS/NZS 1170.0:2002, Standards Association of Australia, Sydney, Australia.

[40] EC0. Eurocode 0: basis of structural design. EN 1990:2002+A1:2005. Brussels, Belgium: European committee for standardization, 2005.

Table 1: Material properties of TSS at elevated temperatures [35]

Steel grades	T_m (°C)	E (GPa)	$f_{0.2}$ (MPa)	f_u (MPa)	ε_u (%)	ε_f (%)
G550	22.0	228	730	743	0.5	2.9
	296.8	215	585	673	3.3	10.1
	457.9	125	290	371	2.2	10.1
	602.0	105	59	88	14.1	51.3
	898.6	6.5	24	46	5.2	11.8
G450	22.0	213	512	543	7.2	15.9
	295.9	209	465	543	5.6	18.5
	457.3	120	266	297	2.1	26.0
	601.3	109	57	87	12.0	59.7
	902.8	42	25	34	4.8	20.3

Note: 22.0 represents the ambient temperature in the lab.

Table 2: Design of TSS single shear bolted connection specimens

Steel grades	t (mm)	d (mm)	e_l	T (°C)
G550	0.42	8	1.0d, 2.0d, 3.0d, and 5.0d	22, 300, 450, 600 and 900
G450	1.90			

Table 3: Effects of end distance on TSS single shear bolted connections at 22 °C

Specimens	$P_{u,r}$ (kN)	$P_{u,r}/P_{AS/NZS}$	$P_{u,r}/P_{NAS}$	$P_{u,r}/P_{EC}$	Failure mode			
					Test	AS/NZS	NAS	EC
042-S-d	2.47	0.88	1.68	1.41	T	T	T	B
042-S-2d	5.45	0.98	1.13	1.56	T	T	T	B
042-S-2d-r	5.42	0.97	1.12	1.55	T	T	T	B
042-S-3d	6.12	0.95	0.95	1.17	B	B	B	B
042-S-5d	5.91	0.92	0.92	1.13	B	B	B	B
042-S-5d-r	6.01	0.94	0.94	1.15	B	B	B	B
042-S-5d-r[#]	5.77	0.90	0.90	1.10	B	B	B	B
190-S-d	7.57	0.91	1.73	1.09	T	T	T	B
190-S-2d	17.25	1.03	1.19	1.23	T	T	T	B
190-S-3d	23.48	0.95	0.97	1.14	B	T + B	T	B
190-S-5d	24.27	0.97	0.97	1.16	B	B	B	B
Mean		0.94	1.14	1.24				
COV		0.044	0.262	0.142				

Note: "#" indicating second repeat test; T = Tearout; B = Bearing.

Table 4: Effects of end distance on TSS single shear bolted connections at 300 °C

Specimens	T_m	$P_{u,h}$	$P_{u,h}/P_{AS/NZS}$	$P_{u,h}/P_{NAS}$	$P_{u,h}/P_{EC}$	Failure mode			
	(°C)	(kN)				Test	AS/NZS	NAS	EC
042-S-d	299.4	2.14	0.85	1.61	1.35	T	T	T	B
042-S-2d	305.5	4.57	0.90	1.05	1.44	T	T	T	B
042-S-3d	302.8	4.79	0.82	0.82	1.01	B	B	B	B
042-S-5d	296.4	4.68	0.80	0.80	0.99	B	B	B	B
190-S-d	307.2	7.77	0.93	1.77	1.12	T	T	T	B
190-S-2d	300.5	17.87	1.07	1.24	1.29	T	T	T	B
190-S-3d	304.5	21.98	0.88	0.90	1.05	B	T + B	T	B
190-S-5d	303.1	22.81	0.91	0.91	1.09	B	B	B	B
Mean			0.90	1.14	1.17				
COV			0.093	0.326	0.146				

Table 5: Effects of end distance on TSS single shear bolted connections at 450 °C

Specimens	T_m	$P_{u,h}$	$P_{u,h}/P_{AS/NZS}$	$P_{u,h}/P_{NAS}$	$P_{u,h}/P_{EC}$	Failure mode			
	(°C)	(kN)				Test	AS/NZS	NAS	EC
042-S-d	448.4	1.75	1.25	2.39	2.01	T	T	T	B
042-S-2d	452.8	3.52	1.26	1.46	2.02	T	T	T	B
042-S-3d	456.9	3.87	1.21	1.21	1.48	B	B	B	B
042-S-5d	454.7	3.84	1.20	1.20	1.47	B	B	B	B
190-S-d	451.2	6.27	1.37	2.62	1.65	T	T	T	B
190-S-2d	447.8	12.45	1.36	1.58	1.64	T	T	T	B
190-S-3d	458.5	13.31	0.97	1.00	1.17	B	T + B	T	B
190-S-5d	452.3	16.42	1.20	1.20	1.44	B	B	B	B
Mean			1.23	1.58	1.61				
COV			0.102	0.379	0.180				

Table 6: Effects of end distance on TSS single shear bolted connections at 600 °C

Specimens	T_m (°C)	$P_{u,h}$ (kN)	$P_{u,h}/P_{AS/NZS}$	$P_{u,h}/P_{NAS}$	$P_{u,h}/P_{EC}$	Failure mode			
						Test	AS/NZS	NAS	EC
042-S-d	599.8	1.19	3.60	6.85	5.75	T	T	T	B
042-S-2d	601.6	1.30	1.96	2.28	3.14	T	T	T	B
042-S-2d-r	602.9	1.24	1.87	2.17	3.00	T	T	T	B
042-S-3d	603.7	1.18	1.55	1.55	1.90	B	B	B	B
042-S-5d	603.9	1.22	1.60	1.60	1.97	B	B	B	B
190-S-d	602.1	1.87	1.40	2.67	1.68	T	T	T	B
190-S-2d	599.5	3.95	1.48	1.71	1.77	T	T	T	B
190-S-3d	601.2	4.84	1.21	1.24	1.45	B	T + B	T	B
190-S-3d-r	600.9	4.55	1.13	1.16	1.36	B	T + B	T	B
190-S-5d	607.6	4.66	1.16	1.16	1.39	B	B	B	B
190-S-5d-r	603.9	4.62	1.15	1.15	1.38	B	B	B	B
Mean			1.65	2.14	2.25				
COV			0.429	0.767	0.583				

Table 7: Effects of end distance on TSS single shear bolted connections at 900 °C

Specimens	T_m	$P_{u,h}$	$P_{u,h}/P_{AS/NZS}$	$P_{u,h}/P_{NAS}$	$P_{u,h}/P_{EC}$	Failure mode			
	(°C)	(kN)				Test	AS/NZS	NAS	EC
042-S-d	900.8	0.37	2.14	4.07	3.42	T	T	T	B
042-S-2d	901.7	0.45	1.30	1.51	2.08	T	T	T	B
042-S-3d	901.7	0.47	1.18	1.18	1.45	B	B	B	B
042-S-5d	899.5	0.44	1.11	1.11	1.36	B	B	B	B
190-S-d	899.5	0.95	1.82	3.46	2.18	T	T	T	B
190-S-2d	897.4	1.42	-	-	-	BS	-	-	-
190-S-3d	900.5	1.21	-	-	-	BS	-	-	-
190-S-3d-r	901.7	1.56	-	-	-	BS	-	-	-
190-S-5d	896.4	1.55	-	-	-	BS	-	-	-
Mean			1.51	2.27	2.20				
COV			0.297	0.616	0.394				

Note: BS = Bolt shear.

Table 8: Effects of end distance on TSS bolted connections at elevated temperatures

Specimen series	Total number		$P_{u,r}/P_{AS/NZS}$ ($P_{u,h}/P_{AS/NZS}$)	$P_{u,r}/P_{NAS}$ ($P_{u,h}/P_{NAS}$)	$P_{u,r}/P_{EC}$ ($P_{u,h}/P_{EC}$)
042-S & 190-S	47	Mean, P_m	1.23	1.61	1.66
		COV, V_p	0.397	0.669	0.509
		Resistance factor, ϕ_1	0.60	0.60	0.80
		Reliability index, β_1	2.51	2.05	2.09
		Resistance factor, ϕ_2	0.60	0.60	0.60
		Reliability index, β_2	2.62	2.05	2.66
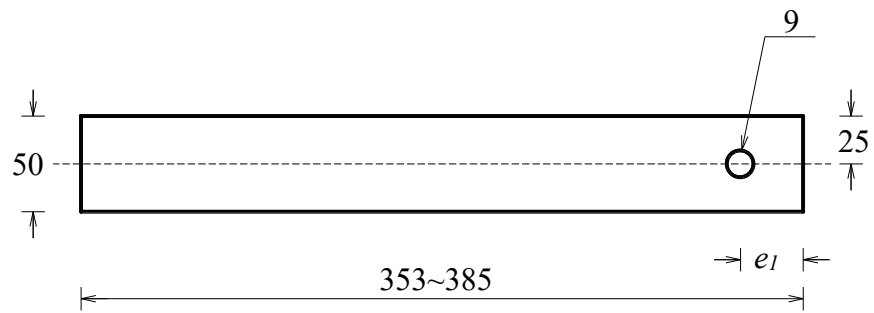
Fig. 1. Values (in mm) and symbols in the connection plates
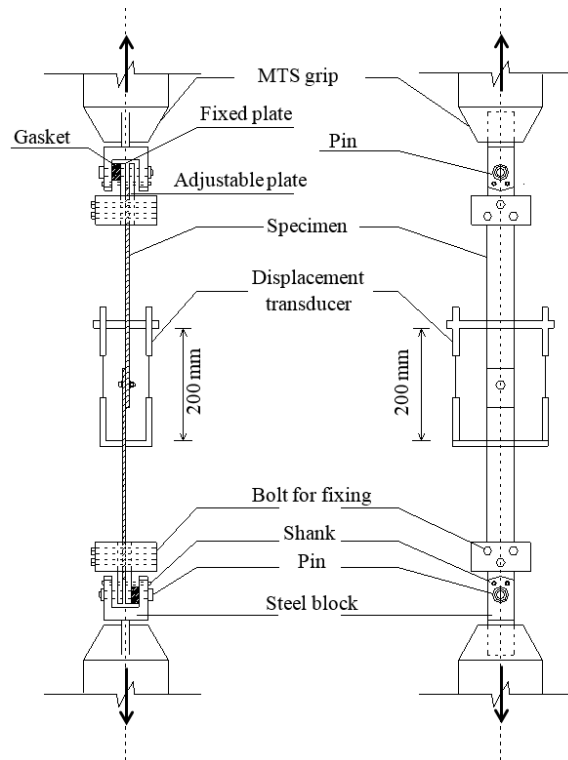
a) Schematic view [38]
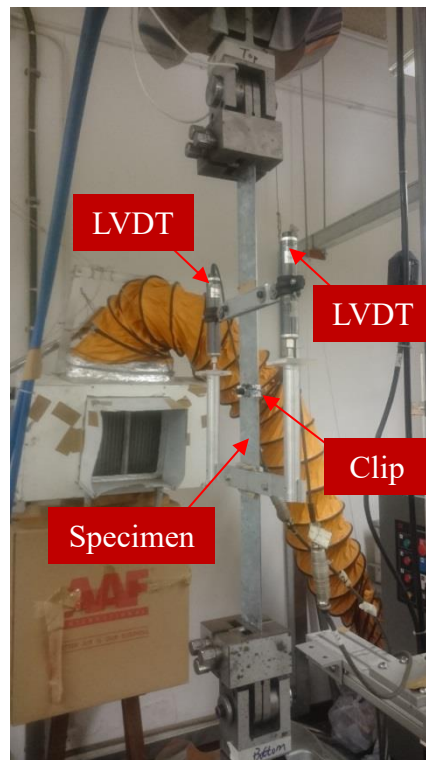
b) Over view of test Specimen 190-S-d

Fig. 2. Test setup of TSS single shear bolted conneciton at ambient temperature condition
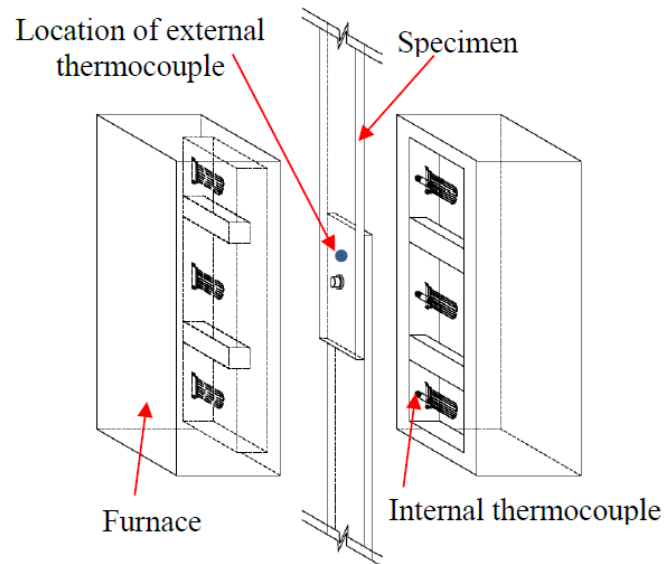
a) Schematic view at high temperature condition
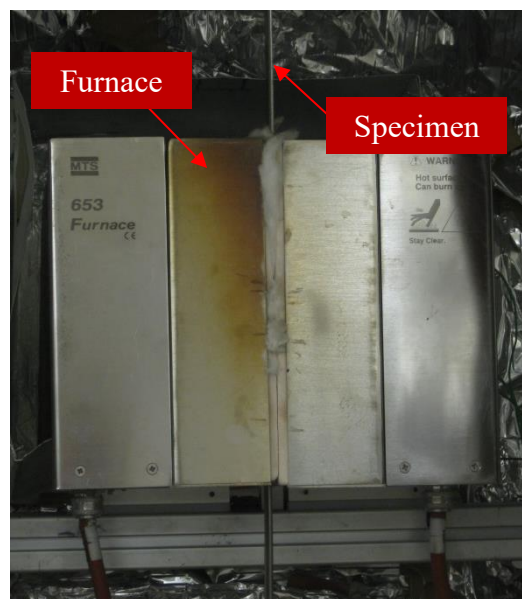
b) Specimen 190-S-3d at 600 °C

Fig. 3. Test setup of TSS single shear bolted conneciton at high temperatures
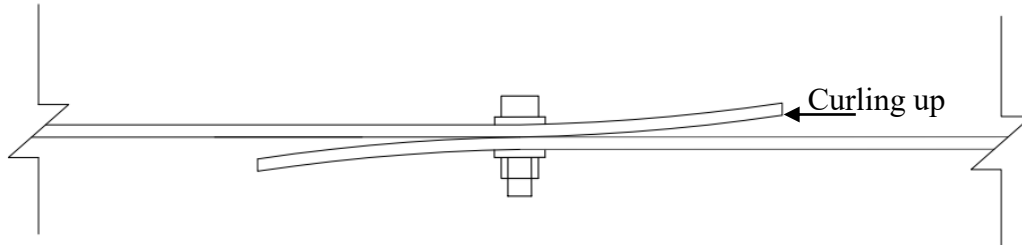
Fig. 4. Curling up of TSS single shear bolted connection specimen
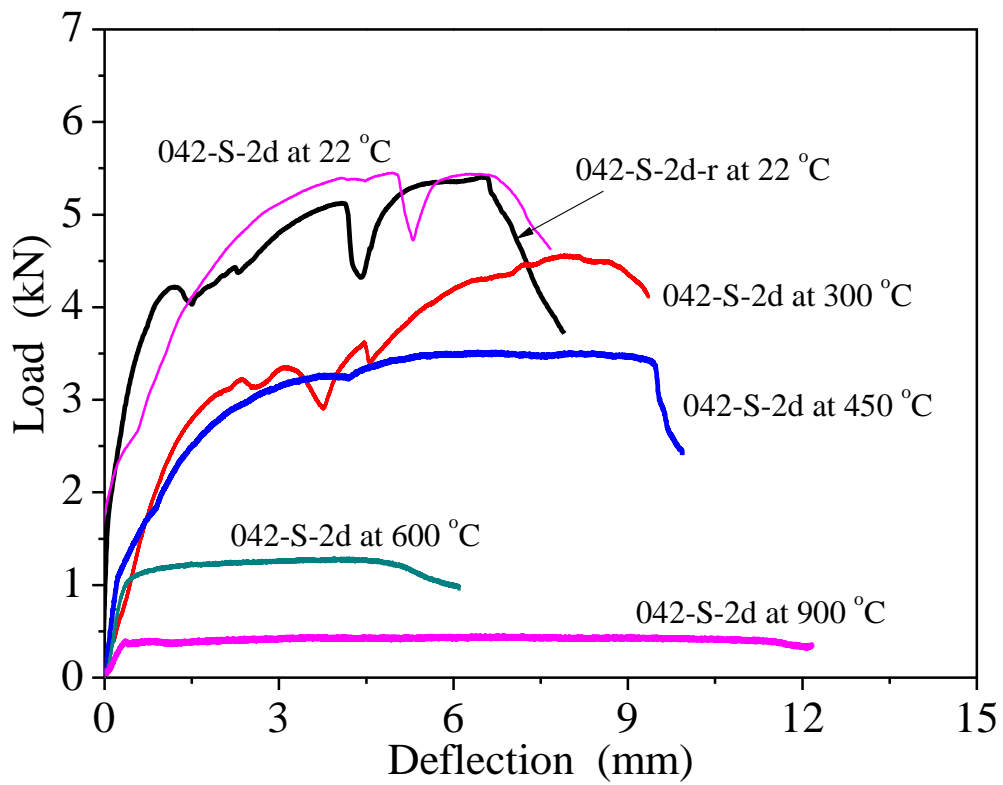
Fig. 5. Load-deflection curves of specimen Series 042-S-2d at elevated temperatures
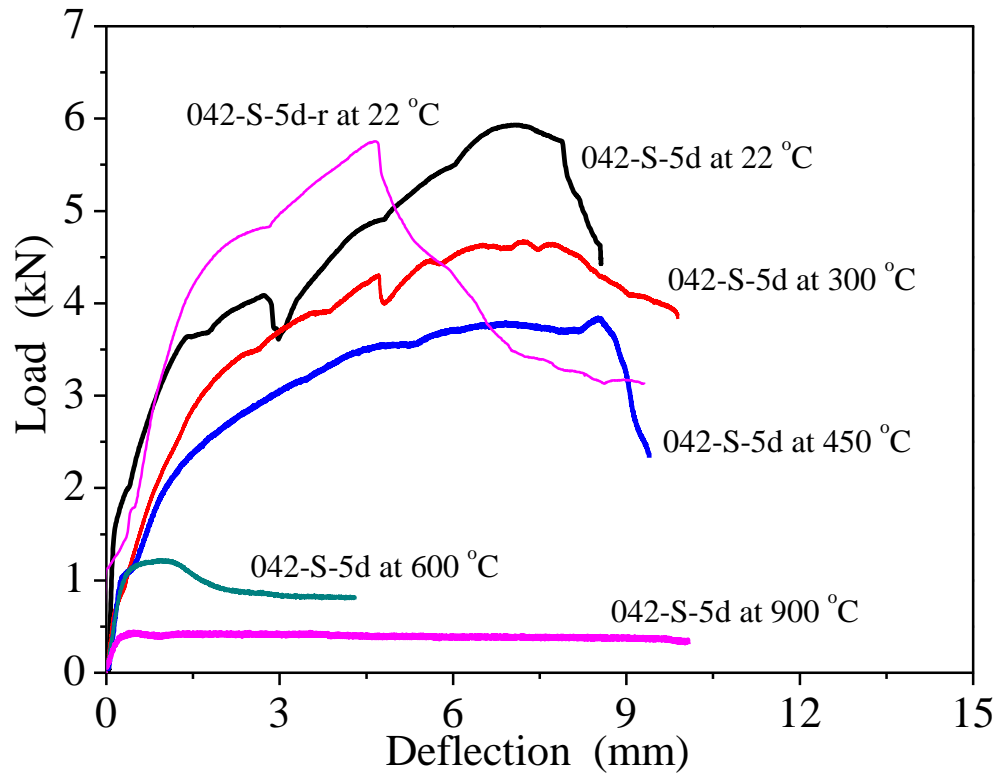
Fig. 6. Load-deflection curves of specimen Series 042-S-5d at elevated temperatures
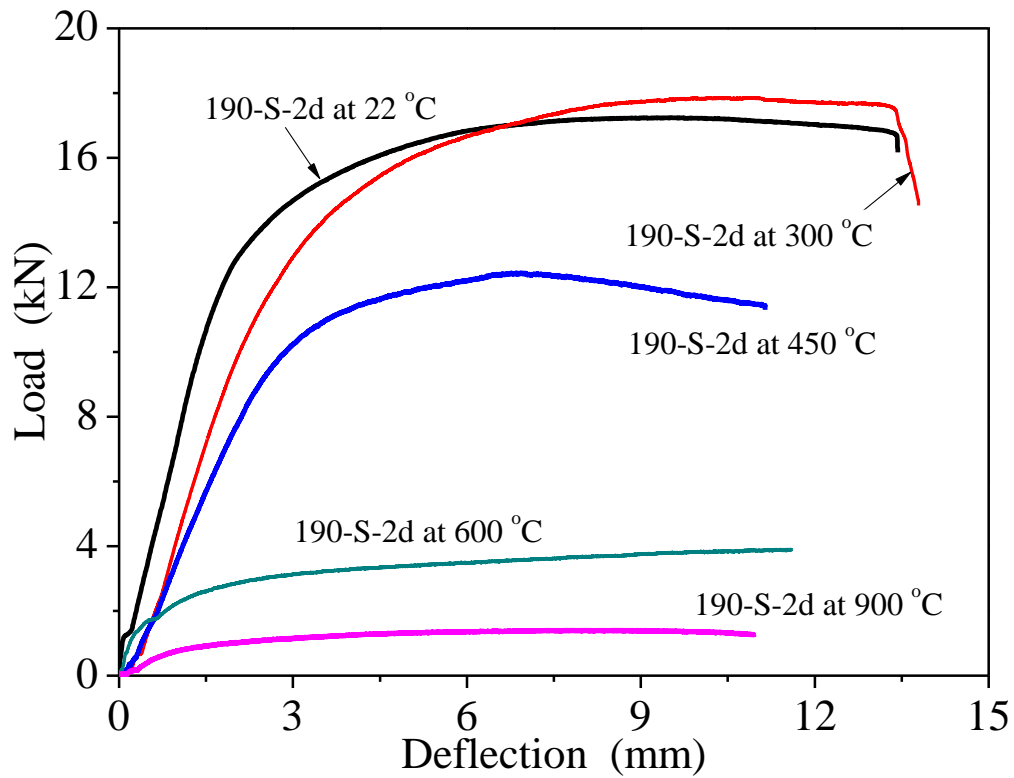
Fig. 7. Load-deflection curves of specimen Series 190-S-2d at elevated temperatures
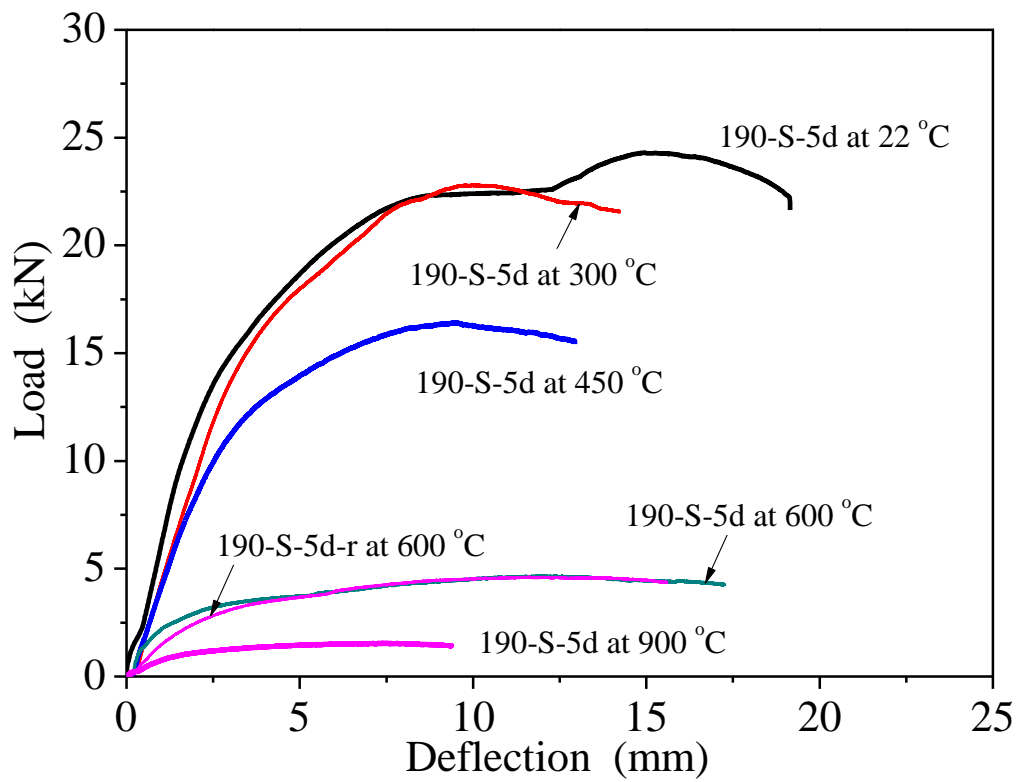
Fig. 8. Load-deflection curves of specimen Series 190-S-5d at elevated temperatures

(a) 042-S-d
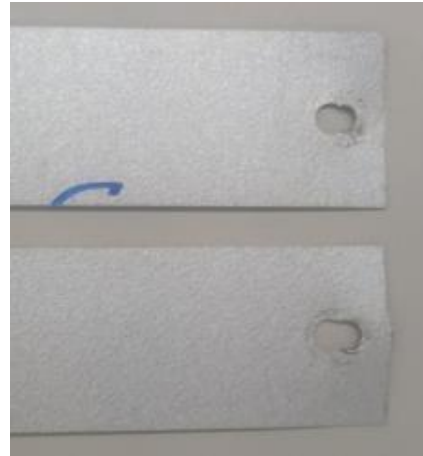
(b) 042-S-2d
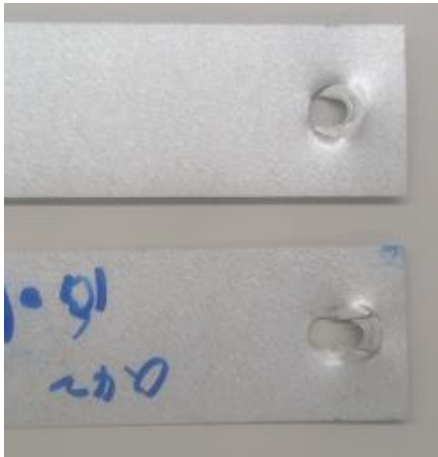
(c) 042-S-3d
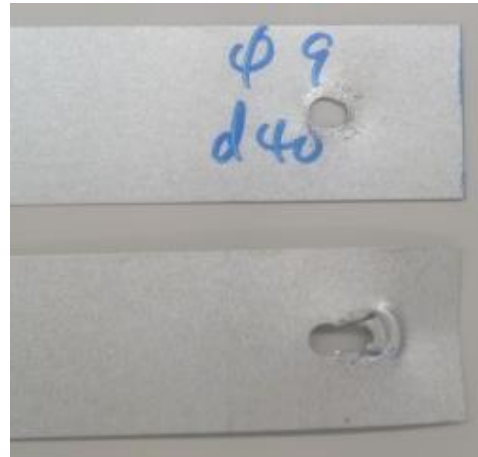
(d) 042-S-5d

Fig. 9. Effects of end distance on failure modes of specimen Series 042-S at ambient temperature

(a) 190-S-d

(b) 190-S-2d
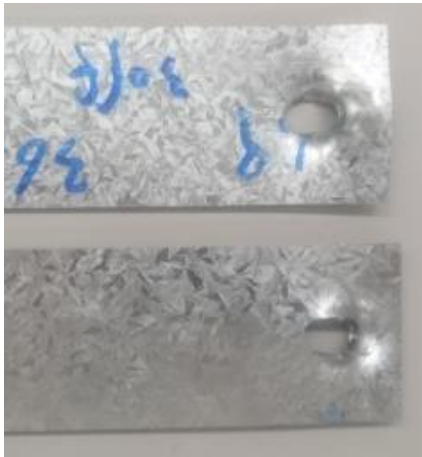
(c) 190-S-3d

(d) 190-S-5d

Fig. 10. Effects of end distance on failure modes of specimen Series 190-S at ambient temperature
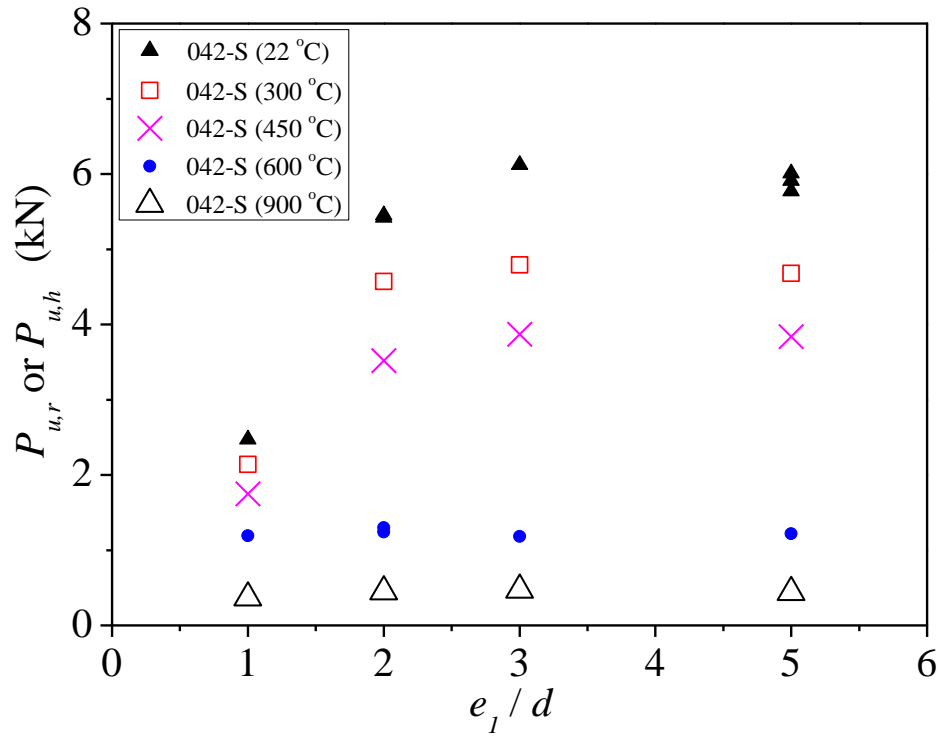
Fig. 11. Effects of end distance on connection specimens Series 042-S at elevated temperatures
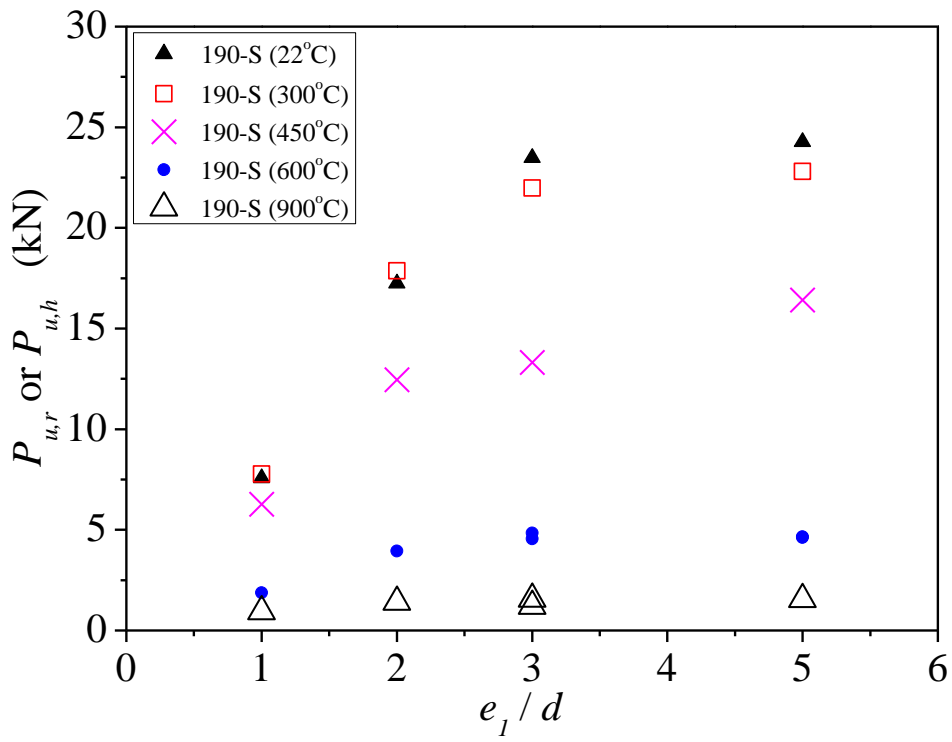
Fig. 12. Effects of end distance on connection specimens Series 190-S at elevated temperatures

(a) 300 °C

(b) 450 °C

(c) 600 °C

(d) 900 °C

Fig. 13. Effects of temperature on failure modes of specimen Series 042-S-d

(a) 300 °C

(b) 450 °C
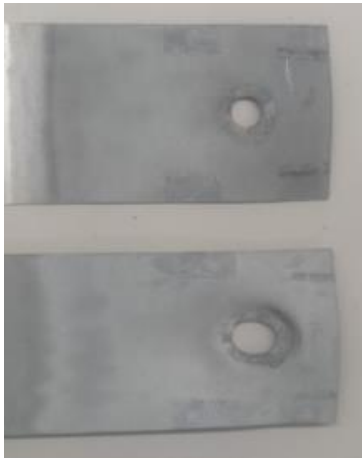
(c) 600 °C
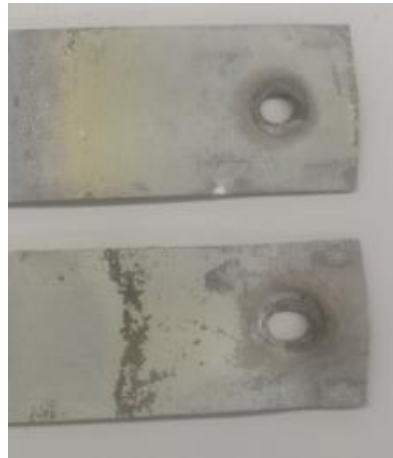
(d) 900 °C

Fig. 14. Effects of temperature on failure modes of specimen Series 042-S-3d

(a) 300 °C

(b) 450 °C

(c) 600 °C

(d) 900 °C

Fig. 15. Effects of temperature on failure modes of specimen Series 190-S-d
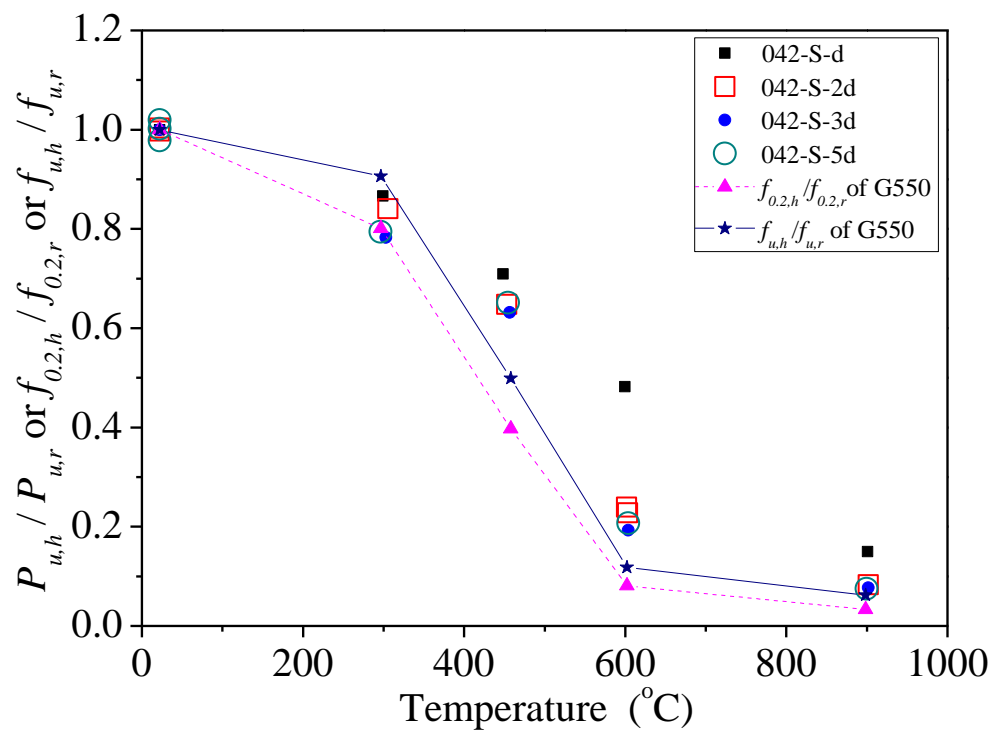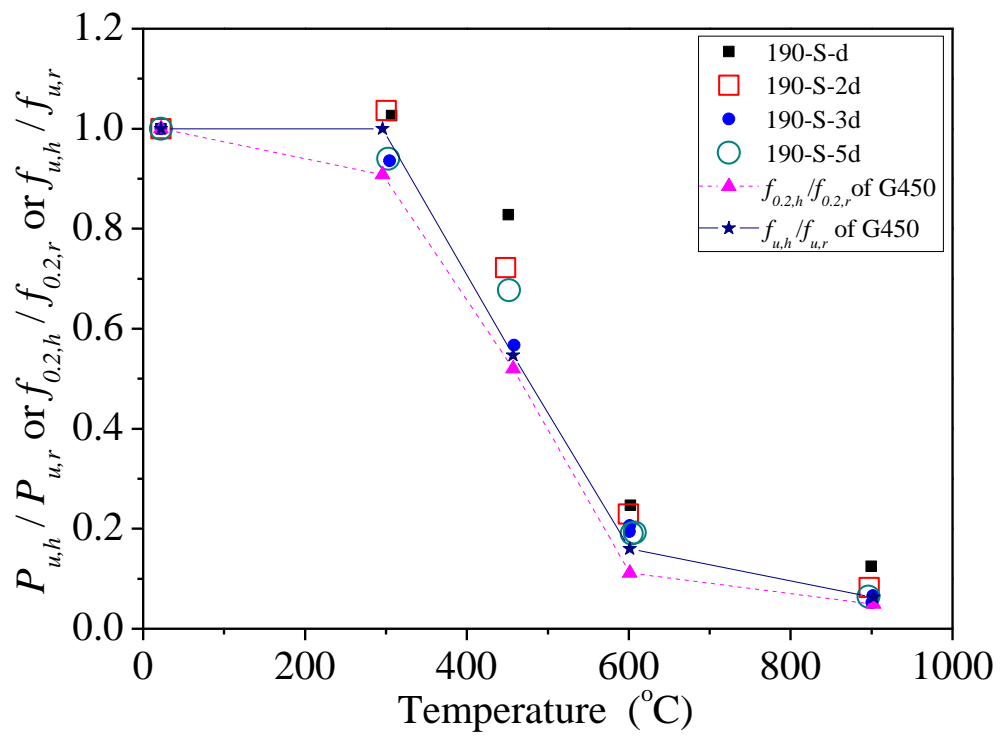
(a) 300 °C   (b) 450 °C
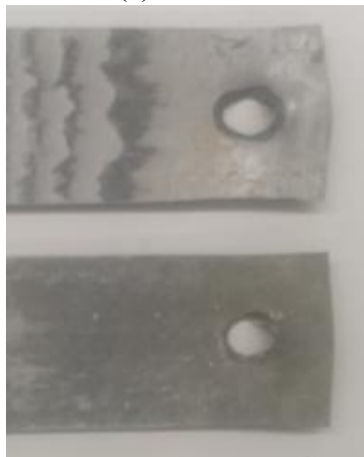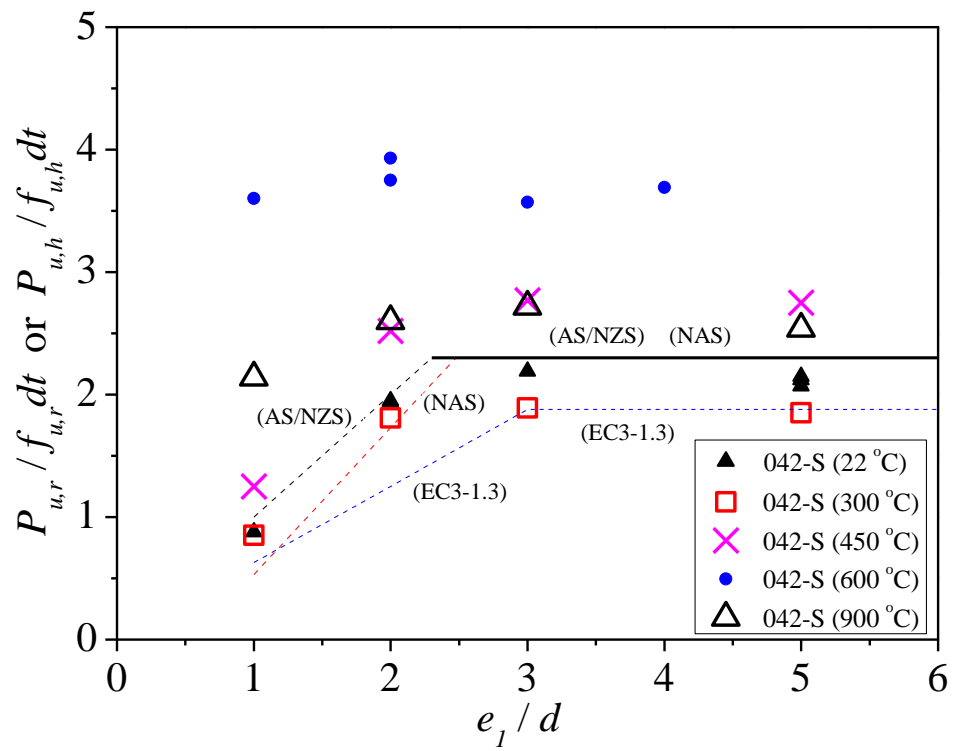
(c) 600 °C   (d) 900 °C

Fig. 16. Effects of temperature on failure modes of specimen Series 190-S-3d
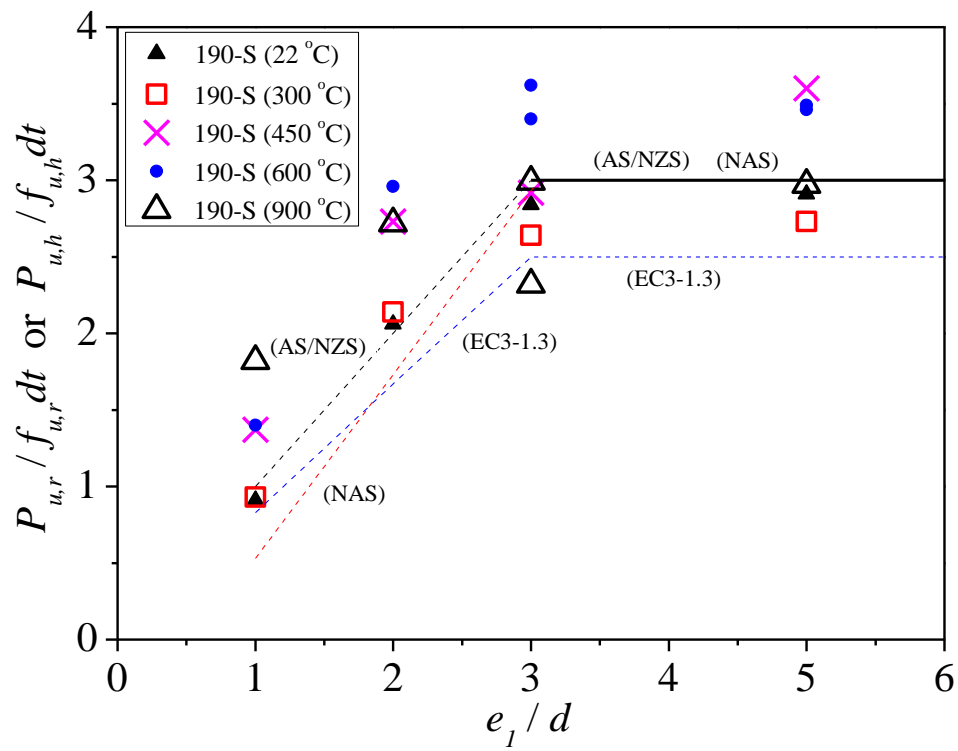
Fig. 17. Effects of temperature on connection specimen Series 042-S

Fig. 18. Effects of temperature on connection specimen Series 190-S

Fig. 19. Comparison of test results with predicted strengths for specimen Series 042-S

Fig. 20. Comparison of test results with predicted strengths for specimen Series 190-S